Proprioceptive Sensor Dataset for Quadrupeds

Geoff Fink and Claudio Semini

Dynamic Legged Systems Lab, Istituto Italiano di Tecnologia (IIT)

Via Morego 30, 16163, Genova, Italy

E-mail: {geoff.fink,claudio.semini}@iit.it

Abstract—**This paper presents novel datasets of the hydraulically actuated robot HyQ's proprioceptive sensors. The datasets include absolute and relative encoders, force and torque sensors, and MEMS-based and fibre optic-based inertial measurement units (IMUs). Additionally, a motion capture system recorded the ground truth data with millimetre accuracy. In the datasets HyQ was manually controlled to trot in place or move around the laboratory. The sequence includes: forward and backwards motion, side-to-side motion, zig-zags, yaw motion, and a mix of linear and yaw motion. All of the datasets are at least five minutes long. The aim of these datasets is to test state estimation using only proprioceptive sensors.**

The datasets can be downloaded from https://www.doi.org/10.21227/4vxz-xw05.

Keywords—**Quadruped, dataset, proprioceptive, robotics, IMU, kinematics, state estimation**

I. INTRODUCTION

The development of quadruped robotic platforms is an active area of research in both the public and private sectors [1]–[4]. The higher degrees of freedom provided by legs compared to wheels or tracks allow legged robots to navigate uneven and rough terrain. They are both more mobile and more versatile. However, with the increased mechanical complexity comes an increased difficulty in state estimation and control.

The *state* of a robot is a set of quantities that describes pertinent information about the robot. Typically, for a mobile robot the state will include the position and velocity. Furthermore, it can include information such as forces, torques, centre of masses, or even 3D maps. State estimation is the problem of estimating the state of a robot from sensor data and models. The difficulty of state estimation is often underestimated. Controlling a robot can be relatively easy if the pose of the robot and a map of the environment is known. However, there are no sensors that can directly measure these variables, and the sensors that can partially measure them are corrupted with noise. Further details regarding state estimation for mobile robotics can be found in [5] and [6].

Much of the current literature on state estimation for mobile robotics has been focused on exteroceptive sensors for simultaneous localization and mapping (SLAM) [7], [8], visual odometry [9], [10], visual SLAM [11], and visual-inertial SLAM [12]–[14]. The goal of these works is to provide a non-drifting pose for robot navigation at the task level, however, the main drawbacks of these approaches are the frequencies and delays in many of the sensors used, e.g., camera and lidars. Furthermore, they do not exploit any quadruped model

or quadruped specific sensors because they are often designed to be generic.

There is also a less numerous, but growing body of literature for state estimation of legged robots at the task level. In [15], [16] the authors proposed an EKF-based sensor fusion algorithm combining inertial measurements, leg odometry, stereo vision, and lidar. In [17] the authors proposed an EKF-based sensor fusion algorithm combing inertial measurements, leg odometry, stereo vision, and GPS. In [18] the authors proposed an indirect feedback information filter-based algorithm that fuses IMU, leg odometry, and stereo vision.

Lastly, there is also literature for lower level state estimation using only proprioceptive sensors. In [19] the authors proposed a particle filtering-based sensor fusion algorithm. In [20] and [21] the authors proposed an observability constrained EKF-based and an unscented Kalman filter-based algorithm, respectively. In [2], [22] the authors proposed a cascaded sensor fusion algorithm that separates the attitude estimator from the position and velocity estimator. In [23] the authors proposed a probabilistic foot contact estimation algorithm.

A problem when trying to compare results in the literature is that all of the results are very platform dependent. There are two main solutions to overcome this: standardized benchmarks and standardized datasets. Multiple benchmarks to compare odometry and state estimator algorithms have been proposed for visual and visual-inertial odometry [24]–[26]. Many of these tools can be directly applied to quadruped odometry. Similarly, many datasets have been published for visual and visual-inertial odometry [27], [28]. However, these datasets to do not contain the typical sensors that are presents in quadrupeds, i.e., force and torque sensors; absolute and relative encoders. To the best of the authors' knowledge similar datasets for quadruped robots that contain proprioceptive sensors do not exist.

The main contribution of this paper is a novel dataset collected on board the hydraulically actuated quadruped HyQ [1]. The dataset contains all of HyQ's proprioceptive sensors running at high frequencies for three scenarios. Furthermore, it was collected in a laboratory that has millimetre accurate position ground truth.

II. EXPERIMENTAL SETUP

The experimental platform for this dataset is the robot HyQ. HyQ weighs approximately 90 kg depending on its current sensor suite and has twelve torque-controlled joints powered by hydraulic actuators. The hydraulic actuators allow the robot
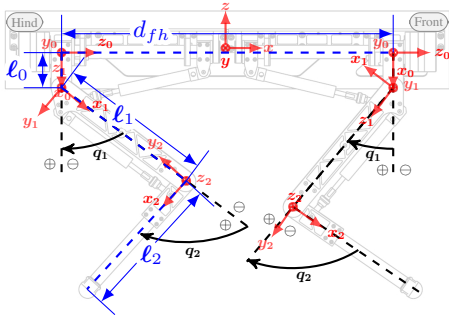
Fig. 1. Diagram of HyQ showing the reference frames for the body and the right legs. The left side is a mirror copy of the right side.

Location	Parameter	Value	Units
trunk	d_{lr}	0.414	m
	d_{fh}	0.747	m
leg	l_0	0.08	m
	l_1	0.35	m
	l_2	0.346	m
	l_3	0.02	m
hip a/a	q_0	$-90 \leq q_0 \leq 30$	°
hip f/e	q_1	$-70 \leq q_1 \leq 50$	°
knee f/e	q_2	$20 \leq q_2 \leq 140$	°

to perform powerful dynamic motions. Detailed mechanical specifications for HyQ are in [1] and [29]. In this paper we highlight some of the relevant geometric parameters of the legs and the joints that are necessary for calculating kinematics of the robot. The four legs are labelled left front (LF), right front (RF), left hind (LH), and right hind (RH). Each leg has three actuated joints: hip abduction/adduction (HAA), Hip flexion/extension (HFE), and knee flexion/extension (KFE). The axis definitions for the trunk and the joints in the RF and RH leg are shown in Fig. 1. The left side is a mirror image of the right such that the following joints have identical coordinate systems: LF_HAA=RH_HAA, LH_HAA=RF_HAA, LF_HFE=RF_HFE, LH_HFE=RH_HFE, LF_KFE=RF_KFE, and LH_KFE=RF_KFE. Also labelled in the figure are the lengths between each joint. The body frame of the robot is located at the geometric centre of the four HAA joints and is orientated such that the x, y, z axes are pointing forward, left, and up, respectively. The geometric parameters of HyQ are in Table I.

There are three important types of proprioceptive sensors on board HyQ: encoders, force/torque sensors, and IMU's. To measure the joint angle each joint contains an absolute and relative encoder. The absolute encoder (AMS Programmable Magnetic Rotary Encoder - AS5045) is used to measure the joint position when the robot is first turned on. Next, the relative encoder (Avago Ultra Miniature, High Resolution Incremental Encoder - AED-3300-TE1) is used to measure how far the joint has moved at every epoch. Also, every joint contains a force or torque sensor. In both the KFE and the HFE there is a load cell (Burster Subminiature Load Cell - 8417-6005) and the HAA has a custom designed torque sensor based on strain-gauges and is similar to [30]. In the trunk of the robot there are two IMUs: a military grade fibre optic KVH-1775 and a MEMS-based high-end consumer grade Lord MicroStrain 3DM-GX5-15. One of the goals of this dataset is to provide an opportunity for researchers to compare the two IMU's using state-of-the-art state estimation algorithms to determine how much the increased accuracy affects drift and if the accuracy is worth the extra cost, size, and weight. All of the sensors are rigidly attached to HyQ with the exception of the 3DM-GX5-15. It has been mounted on top of a 0.25 inch

thick Sorbothane vibration isolation pad. The basis vectors of the GX4 sensor frame are orientated forward, right, and down; and the basis vectors of the KVH sensor frame are orientated right, forward, and down. To measure the ground truth pose of the robot the lab is equipped with a motion capture system (MCS). In particular we use a mix of Vicon T10 and Vero 2 cameras. A summary of the proprioceptive sensors on board HyQ are summarized in Table II.

The first step in using any sensor is proper calibration. The force and torque sensors on board HyQ have external calibrations performed by the manufacturer before being installed. The absolute encoders must be calibrated after they are installed to a known angle. For this purpose a calibration frame that forces all of the legs into the position where $q_0 = q_1 = 0°$ and $q_2 = 90°$. The IMU's are also factory calibrated and do not have a specific offline calibration procedure, however, online bias states should be estimated. The last calibration procedure of importance is the (constant) transformations between the body frame, the IMU sensor frames, and the Vicon marker frame. For both of the IMUs the mounting position of the sensor is known in CAD except for an offset to the GX5 from the Sorbothane vibration isolation pad. The transformation to the Vicon marker is less accurate as it is 3D printed plastic part with a higher tolerance.

The low level software framework runs on an Intel Intense PC 3 with Ubuntu 16 that has been compiled with a real-time kernel patch. The communication between all of the sensors and the motors is based on EtherCAT. The master is programmed using SOEM. The slaves use an EtherCAT controller connected to a microcontroller. This architecture provides a high speed, low latency, and low jitter environment.

III. DATASET

The raw data from all of the datasets described in this paper can be found on the IEEE DataPort Platform [31] with the following DOI: 10.21227/4vxz-xw05. Each of the datasets was recorded on the quadruped robot HyQ indoors at the Dynamic Legged Systems laboratory. The aim of these datasets is to test state estimation using only proprioceptive sensors. For ground truth the lab is equipped with a MCS that records the pose of the robot with millimetre accuracy. Each of the datasets comprises of the raw sensor data of all the sensors

TABLE II
TECHNICAL SPECIFICATIONS OF THE PROPRIOCEPTIVE SENSORS.

Encoders			
	AS5045	AED-3300-TE1	Units
Resolution	4096	80000	cpr
Accuracy	±0.5	±0.5	deg
Max. Speed	153	1950	rpm
MSF	10	650	kHz
Force/Torque Sensors			
	8417-6005	Custom	Units
Range	$0-5000$	±200	N, Nm
Resolution‡	16	16	bits
Inertial Measurement Units (IMUs)			
	KVH-1775	3DM-GX5-15	Units
Technology	Fibre optics	MEMS	-
Gyroscope			
Input Limit	490	300	deg/sec
TBI	0.05	8	deg/hr
Rand. Walk	0.7	18	$\frac{deg}{hr\sqrt{Hz}}$
Bandwidth†	440	250	Hz
MSF	5000	4000	Hz
Accelerometer			
Input Limit	±10	±8	g
TBI	0.05	0.04	mg
Rand. Walk	120	25	$\frac{\mu g}{\sqrt{Hz}}$
Bandwidth	200	225	Hz
MSF	5000	1000	Hz

MSF - Maximum Sampling Frequency
TBI - Typical Bias Instability
† Bandwidth at data rate of 1000 Hz
‡ ADC Resolution

TABLE III
COMPARISON OF DATASETS

Name	Dur.	Dist.	Speed	Rate	Sensors	GT
Trot in Place	349 s	28 m	0.1 m/s	1 kHz	RE,AE,G,A	✓
Trot in Lab 1	374 s	88 m	0.3 m/s	1 kHz	RE,AE,G,A	✓
Trot in Lab 2	344 s	82 m	0.2 m/s	1 kHz	RE,AE,G,A	✓

RE=Relative Encoder, AE=Absolute Encoder, G=Gyroscope
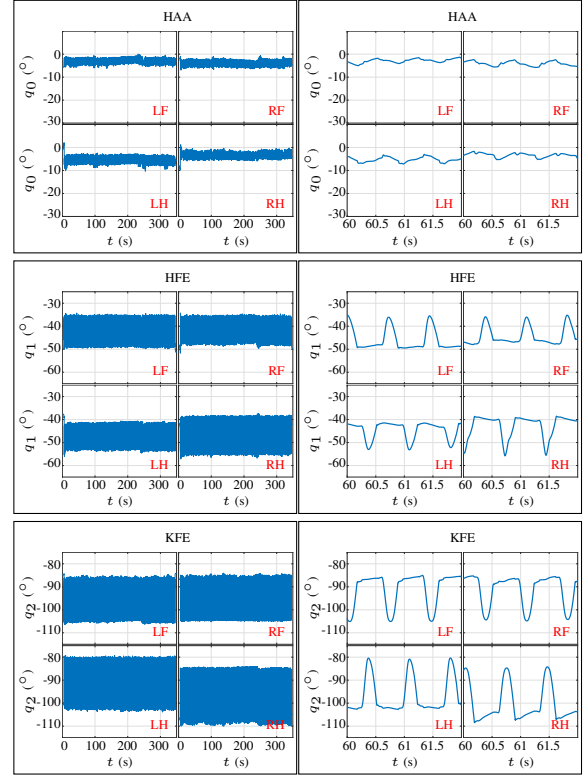A=Accelerometer, GT=Ground Truth)

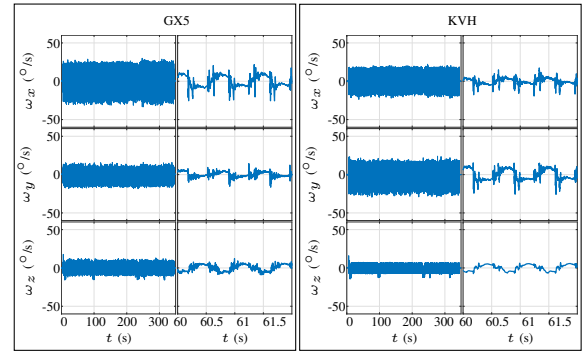Fig. 2. The measured joint positions q in the *trot in place* dataset.

Fig. 3. The measured angular velocity ω in the respective sensors frames for the *trot in place* dataset.

listed in Table II recorded at 1000 Hz and the MCS ground truth recorded at 250 Hz. The data is provided in both comma-separated values and Matlab file format. The data from the sensors and the data from MCS are on two distinct clocks. For convenience a plot of each of the sensors is provided online along side the numerical data.

HyQ has the ability to perform many dynamic gaits, for these datasets we chose to record trotting data as it is representative of a typical quadruped mission. In the first dataset HyQ had to trot in place for more than five minutes. In the following two datasets HyQ was manually controlled by joypad to trot around the laboratory. The sequence includes: forward and backwards motion, side-to-side motion, zig-zags, yaw motion, and a mix of linear, and yaw motion. Both datasets were also at least five minutes long. Fig. 2 shows the joint positions during the *trot in place* dataset. Plots of the other sensors are not shown due to space restrictions, but are available online alongside the raw data. A summary of the datasets is shown in Table III.
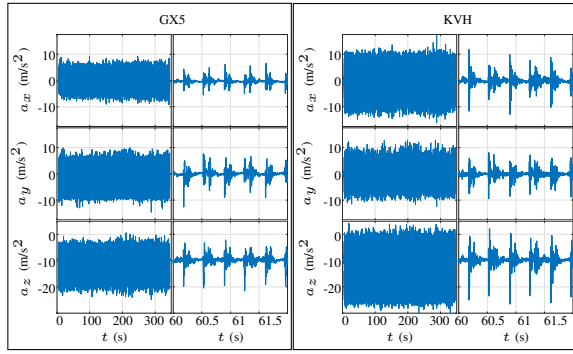
Fig. 4. The measured specific force a in the respective sensors frames for the *trot in place* dataset.
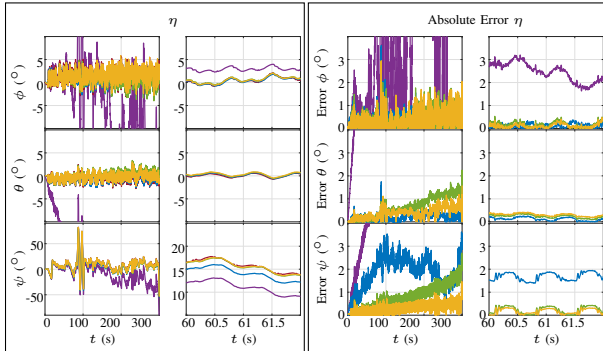

Fig. 5. The estimated trunk attitude by the GX5 AHRS (blue), the integral of the GX5 angular velocity with the bias removed and without the bias removed (green and purple, respectively), the integral of the KVH angular velocity (yellow), and the ground truth from the MCS (red) for the *Trot in Lab 1* dataset.

IV. DISCUSSION

One of the important tasks of state estimation using proprioceptive sensors is attitude estimation. The simplest method to calculate attitude is to integrate the angular velocity starting at a known value. Note that we expect this value to drift due to the noise in the sensors and from bias instability. Furthermore, this value is a worst case scenario as it does not include sensor fusion nor known noise characteristics. However, it does provide a base comparison for the two sensors. Fig. 3 and Fig. 4 show the angular velocity and specific force, respectively, measured in the sensor frame. A comparison of the attitude provided by the ground truth (Vicon), the estimated attitude via integration of the angular velocity by both IMU's, and the estimated attitude via the GX5's onboard AHRS is shown in Fig. 5. We denote the orientation using the XYZ Euler angles $\eta = [\phi, \theta, \psi]^T$. The plot shows the advantage of a fibre optic gyroscope, but we expect the drift of both IMU's to decrease after sensor fusion. Furthermore, the plots help demonstrate the difficulty in attitude estimation when there are large impacts and vibrations.

V. CONCLUSION

In this work we presented a novel dataset collected on board the hydraulically actuated quadruped HyQ. The dataset contains all of HyQ's proprioceptive sensors running at high frequencies for three scenarios. Additionally, the dataset contains precise ground truth data. We believe that this dataset will be highly useful to all researchers working on state estimation for quadruped robots. Future work includes expanding the dataset to include more gaits and different terrains. Furthermore, we will use these datasets to benchmark our future state estimation algorithms.

REFERENCES

[1] C. Semini, N. G. Tsagarakis, E. Guglielmino, M. Focchi, F. Cannella, and D. G. Caldwell, "Design of HyQ – a hydraulically and electrically actuated quadruped robot," *Proc. Inst. Mech. Eng. I J. Syst. Control Eng.*, vol. 225, no. 6, pp. 831–849, 2011, DOI:10.1177/0959651811402275.

[2] G. Bledt, M. J. Powell, B. Katz, J. Di Carlo, P. M. Wensing, and S. Kim, "MIT Cheetah 3: Design and control of a robust, dynamic quadruped robot," in *Int. Conf. on Intell. Robots and Syst. (IROS)*, Madrid, Spain, Oct. 2018, pp. 2245–2252, DOI:10.1109/IROS.2018.8593885.

[3] M. Hutter, C. Gehring, D. Jud, A. Lauber, C. D. Bellicoso, V. Tsounis, J. Hwangbo, K. Bodie, P. Fankhauser, M. Bloesch, R. Diethelm, S. Bachmann, A. Melzer, and M. Hoepflinger, "ANYmal - a highly mobile and dynamic quadrupedal robot," in *Int. Conf. on Intell. Robots and Syst. (IROS)*, Daejeon, South Korea, Oct. 2016, pp. 38–44, DOI:10.1109/IROS.2016.7758092.

[4] M. Raibert, K. Blankespoor, G. Nelson, and R. Playter, "Big-Dog, the rough-terrain quadruped robot," *IFAC Proceedings Volumes*, vol. 41, no. 2, pp. 10 822–10 825, 2008, DOI:10.3182/20080706-5-KR-1001.01833.

[5] S. Thrun, W. Burgard, and D. Fox, *Probabilistic Robotics (Intelligent Robotics and Autonomous Agents)*. Cambridge, MA: The MIT Press, 2005.

[6] T. D. Barfoot, *State Estimation for Robotics*. Cambridge, United Kingdom: Cambridge University Press, 2017, DOI:10.1017/9781316671528.

[7] H. Durrant-Whyte and T. Bailey, "Simultaneous localization and mapping: part I," *IEEE Robot. Autom. Mag.*, vol. 13, no. 2, pp. 99–110, Jun. 2006, DOI:10.1109/MRA.2006.1638022.

[8] T. Bailey and H. Durrant-Whyte, "Simultaneous localization and mapping (SLAM): part II," *IEEE Robot. Autom. Mag.*, vol. 13, no. 3, pp. 108–117, Sep. 2006, DOI:10.1109/MRA.2006.1678144.

[9] D. Scaramuzza and F. Fraundorfer, "Visual odometry [tutorial]," *IEEE Robot. Autom. Mag.*, vol. 18, no. 4, pp. 80–92, Dec. 2011, DOI:10.1109/MRA.2011.943233.

[10] F. Fraundorfer and D. Scaramuzza, "Visual odometry : Part II: Matching, robustness, optimization, and applications," *IEEE Robot. Autom. Mag.*, vol. 19, no. 2, pp. 78–90, Jun. 2012, DOI:10.1109/MRA.2012.2182810.

[11] A. J. Davison, I. D. Reid, N. D. Molton, and O. Stasse, "MonoSLAM: Real-time single camera SLAM," *IEEE Trans. Pattern Anal. Mach. Intell.*, vol. 29, no. 6, pp. 1052–1067, Jun. 2007, DOI:10.1109/TPAMI.2007.1049.

[12] A. Concha, G. Loianno, V. Kumar, and J. Civera, "Visual-inertial direct SLAM," in *IEEE Int. Conf. Robot. Autom. (ICRA)*, Stockholm, Sweden, May 2016, pp. 1331–1338, DOI:10.1109/ICRA.2016.7487266.

[13] T. Pire, R. Baravalle, A. D'Alessandro, and J. Civera, "Real-time dense map fusion for stereo SLAM," *Robotica*, vol. 36, no. 10, pp. 1510–1526, 2018, DOI:10.1017/S0263574718000528.

[14] J. Engel, J. Sturm, and D. Cremers, "Scale-aware navigation of a low-cost quadrocopter with a monocular camera," *Robotics and Autonomous Systems*, vol. 62, no. 11, pp. 1646–1656, 2014, special Issue on Visual Control of Mobile Robots. DOI:10.1016/j.robot.2014.03.012.

[15] S. Nobili, M. Camurri, V. Barasuol, M. Focchi, D. Caldwell, C. Semini, and M. Fallon, "Heterogeneous sensor fusion for accurate state estimation of dynamic legged robots," in *Proc. of Robot.: Sci. and Syst. (RSS)*, Cambridge, Massachusetts, Jul. 2017, pp. 1–9, DOI:10.15607/RSS.2017.XIII.007.

[16] M. Camurri, M. Fallon, S. Bazeille, A. Radulescu, V. Barasuol, D. G. Caldwell, and C. Semini, "Probabilistic contact estimation and impact detection for state estimation of quadruped robots," *IEEE Robot. Autom. Lett.*, vol. 2, no. 2, pp. 1023–1030, Apr. 2017, DOI:10.1109/LRA.2017.2652491.

[17] J. Ma, M. Bajracharya, S. Susca, L. Matthies, and M. Malchano, "Real-time pose estimation of a dynamic quadruped in GPS-denied environments for 24-hour operation," *Int. J. of Robotics Res.*, vol. 35, no. 6, pp. 631–653, 2016, DOI:10.1177/0278364915587333.

[18] A. Chilian, H. Hirschmüller, and M. Görner, "Multisensor data fusion for robust pose estimation of a six-legged walking robot," in *Int. Conf. on Intell. Robots and Syst. (IROS)*, San Francisco, CA, Sep. 2011, pp. 2497–2504, DOI:10.1109/IROS.2011.6094484.

[19] S. Chitta, P. Vernaza, R. Geykhman, and D. D. Lee, "Proprioceptive localilzatilon for a quadrupedal robot on known terrain," in *IEEE Int. Conf. Robot. Autom. (ICRA)*, Roma, Italy, Apr. 2007, pp. 4582–4587, DOI:10.1109/ROBOT.2007.364185.

[20] M. Bloesch, M. Hutter, M. Hoepflinger, S. Leutenegger, C. Gehring, C. D. Remy, and R. Siegwart, "State estimation for legged robots - consistent fusion of leg kinematics and IMU," in *Proc. of Robot.: Sci. and Syst. (RSS)*, Sydney, Australia, Jul. 2012, pp. 1–8, DOI:10.15607/RSS.2012.VIII.003.

[21] M. Bloesch, C. Gehring, P. Fankhauser, M. Hutter, M. A. Hoepflinger, and R. Siegwart, "State estimation for legged robots on unstable and slippery terrain," in *Int. Conf. on Intell. Robots and Syst. (IROS)*, Tokyo, Japan, Nov. 2013, pp. 6058–6064, DOI:10.1109/IROS.2013.6697236.

[22] T. Flayols, A. Del Prete, P. Wensing, A. Mifsud, M. Benallegue, and O. Stasse, "Experimental evaluation of simple estimators for humanoid robots," in *IEEE RAS Int. Conf. on Humanoid Robots (Humanoids)*, Birmingham, UK, Nov. 2017, pp. 889–895, DOI:10.1109/HUMANOIDS.2017.8246977.

[23] J. Hwangbo, C. D. Bellicoso, P. Fankhauser, and M. Hutter, "Probabilistic foot contact estimation by fusing information from dynamics and differential/forward kinematics," in *Int. Conf. on Intell. Robots and Syst. (IROS)*, Daejeon, South Korea, Oct. 2016, pp. 3872–3878, DOI:10.1109/IROS.2016.7759570.

[24] J. Delmerico and D. Scaramuzza, "A benchmark comparison of monocular visual-inertial odometry algorithms for flying robots," in *IEEE Int. Conf. Robot. Autom. (ICRA)*, Brisbane, Australia, May 2018, pp. 2502–2509, DOI:10.1109/ICRA.2018.8460664.

[25] A. Geiger, P. Lenz, and R. Urtasun, "Are we ready for autonomous driving? the KITTI vision benchmark suite," in *Conf. on Comput. Vision and Pattern Recog. (CVPR)*, Providence, RI, Jun. 2012, pp. 3354–3361, DOI:10.1109/CVPR.2012.6248074.

[26] D. Schubert, T. Goll, N. Demmel, V. Usenko, J. Stückler, and D. Cremers, "The TUM VI benchmark for evaluating visual-inertial odometry," in *Int. Conf. on Intell. Robots and Syst. (IROS)*, Madrid, Spain, Oct. 2018, pp. 1680–1687, DOI:10.1109/IROS.2018.8593419.

[27] M. Burri, J. Nikolic, P. Gohl, T. Schneider, J. Rehder, S. Omari, M. W. Achtelik, and R. Siegwart, "The EuRoC micro aerial vehicle datasets," *Int. J. of Robotics Res.*, vol. 35, no. 10, pp. 1157–1163, 2016, DOI:10.1177/0278364915620033.

[28] A. Geiger, P. Lenz, C. Stiller, and R. Urtasun, "Vision meets robotics: The KITTI dataset," *Int. J. of Robotics Res.*, vol. 32, no. 11, pp. 1231–1237, 2013, DOI:10.1177/0278364913491297.

[29] C. Semini, "HyQ - design and development of a hydraulically actuated quadruped robot," Ph.D. dissertation, University of Genoa and Italian Institute of Technology (IIT), Genoa, Italy, Apr. 2010.

[30] H. Khan, M. D'Imperio, F. Cannella, D. G. Caldwell, A. Cuschieri, and C. Semini, "Towards scalable strain gauge-based joint torque sensors," *Sensors*, vol. 17, no. 8, pp. 1–17, 2017, DOI:10.3390/s17081905.

[31] G. Fink, *Proprioceptive Sensor Dataset for Quadruped Robots*. IEEE Dataport, 2019, DOI:10.21227/4vxz-xw05.